Applied Clay Science 250 (2024) 107284

Contents lists available at ScienceDirect

Applied Clay Science

journal homepage: www.elsevier.com/locate/clay

Research Paper

Statistical significance of curing variables on geopolymerization of mining by-product untreated clay

Caterina Sgarlata [a], Francesco Edoardo Vaccari [b], Alessandra Formia [c], Francesco Ferrari [d], Cristina Leonelli [a,*]

[a] Department of Engineering "Enzo Ferrari", University of Modena and Reggio Emilia, Via Pietro Vivarelli 10, 41125 Modena, Italy
[b] Department of Biomedical and Neuromotor Sciences, Alma Mater Studiorum - University of Bologna, Piazza di Porta San Donato, 2, 40126 Bologna, Italy
[c] Sibelco Ankerpoort NV, Maastricht, the Netherlands
[d] Sibelco Italia S.p.A., Maranello, MO, Italy

ARTICLE INFO

Keywords:
Mining by-product
Halloysite
Geopolymer
Untreated clay
Curing condition
Statistical data treatment

ABSTRACT

The focus of this research is to investigate of the possibility of reusing mineral wastes and by-products from mining processes to produce more sustainable binders in large amounts. A mining by-product consisting of halloysite (approximately 48 wt%) was used to produce dense alkali activated solids. Attention was paid to the influence of temperature on the geopolymerisation process in terms of the microstructural characteristics of the samples obtained. The challenge was to alkali activate the clay as received without any firing pre-treatment. The fresh paste of untreated clay was cured at 50% relative humidity (RH%) at different temperatures: 40, 60, and 70 °C. The halloysite-bearing powder (HC) was then mixed with a low-quartz sand, a second by-product of the mining industry, to achieve higher chemical stability. The results showed a clear difference in chemical stability for samples containing sand compared to those without sand. Low percentages of metakaolin (5–15%) were also added to the same formulations to improve the chemical and physical properties of the samples and to reduce the curing time. For mixtures consisting of untreated clay and sand only NaOH was added as alkaline activator. The effect of curing temperature, curing time and addition of metakaolin (MK) on the microstructure of the geopolymers was analysed by different techniques: measurement of pH and ionic conductivity of the eluate of the chemical stability test in water, X-ray diffraction (XRD), scanning electron microscopy (SEM), bulk density, and compressive strength.

Finally, a statistical approach was adopted to rationalise the effect of the curing conditions on the consolidation of the fresh pastes of samples with the untreated HC, sand and metakaolin. To test whether the parameters of the curing process, as well as the MK addition had an influence on the values of the ionic conductivity of the eluate from water sinking and/or the density of the solid final product, a 3-way ANOVA followed by Tukey-Kramer post hoc tests ($p < 0.05$) were performed. To further investigate the interaction between preparation parameters and the material properties, we also built a Generalized Linear model that provided an equation to predict the final results. Overall, we found that the addition of MK significantly reduced the conductivity while only marginally increasing the density of the material. This effect was extremely temperature-dependent, and it disappeared at 70 °C. In conclusion, it has been demonstrated how the addition of fillers, an easily controllable industrial step, can maximise the performance of the consolidated material, rather than controlling the curing time and temperature conditions.

1. Introduction

In the search for alternatives to Ordinary Portland Cement-OPC, Supplementary Cementitious Materials – SCMs such as fly ash from power plants, slags from metallurgical processes and natural pozzolana (Lothenbach et al., 2011) or, alternatively, Limestone Calcined Clay Cements - LC^3 (Scrivener et al., 2018; Almas et al., 2021; Blouch et al., 2023) containing only 50% of the clinker required to consolidate OPC have been developed. Alkali activation of clay minerals or residues (Žibret et al., 2023) without the use of clinker has also been proposed.

* Corresponding author.
E-mail address: cristina.leonelli@unimore.it (C. Leonelli).

https://doi.org/10.1016/j.clay.2024.107284
Received 10 August 2023; Received in revised form 25 January 2024; Accepted 29 January 2024
Available online 7 February 2024

Some works presented the production of inorganic binders from untreated kaolinite by adding concentrated NaOH solutions (6–12 mol/l). In the case of unfired clay, similar to uncalcined kaolinite, the use of NaOH solution was proposed by Slaty et al. (Slaty et al., 2013), different from the typical procedure with NaOH or KOH added to a silicate solution of K or Na in the case of metakaolin-based formulations. The OH^- concentration of the activator is an important parameter. Alkalinity is primarily required to break down of the aluminosilicate layer (Zhang et al., 2013). As the reactivity of kaolinite, or in this case halloysite, is much lower than that of thermally activated clays, such strong alkaline solutions must be used. Na^+ ions from the activator solution remain in the geopolymer structure as the counter ion to the negative charge introduced by each $(AlO_4)^{5-}$ tetrahedron formed during the hardening/condensation stage (Fernandez et al., 2011). Strictly related to such a stage, the curing process at temperatures between 40 and 100 °C is crucial to enhance the geopolymerisation process (Slaty et al., 2013). The formulations presented here were prepared with a curing temperature of 40 °C, 60 °C and 70 °C, as suggested in the literature (Yousef et al., 2012), for the first 3–7 days, and then left to dry at room temperature for the remaining 21 days, before testing in water.

It has been reported in the literature that the introduction of a percentage of silica sand could lead to improvements in the workability of the mix and an increase in the compressive strength (Esaifan et al., 2015). Due to the low reactivity of the clay studied in this work, the formulations were designed with the addition of a fine silica sand and low percentages of metakaolin. The addition of low percentages of metakaolin (5–15%) has been used in literature as a reactive filler to improve the compressive strength, reduce the setting time of fresh geopolymer paste and the linear shrinkage of hardened geopolymer (Tchakoute Kouamo et al., 2013).

In this study, a halloysitic clay (HC), classified as a mining by-product, was chosen as a starting aluminosilicate powder to investigate the preparation of dense alkali activated solids using only NaOH solution (Sgarlata et al., 2022). According to the literature (Duxson et al., 2005; Wan et al., 2017. Kóth and Sinkó, 2023), the molar ratios of Na/Al and Si/Al to obtain a good structural material were calculated to be around Na/Al = 1–2 and $1 \leq Si/Al \leq 3$. Therefore, we followed this rule for the Si/Al ratio, but we increased the Na/Al ratio slightly above 2, since our intention was to activate unfired clay.

Many formulation hypotheses were developed based on: i) the values of Si/Al and Na/Al molar ratios within the ranges given above, ii) the amount of water to be added, and iii) the curing temperature (Sgarlata, 2022). The first properties tested for a qualitative assessment of the results obtained were the chemical stability in water in terms of sample integrity. In addition, more quantitative tests were carried out, i.e. the determination of the pH and ionic conductivity of the eluate after the immersion of the samples in water.

Attention was focused on the influence of the temperature on the geopolymerisation process, and the influence of metakaolin addition on the chemical stability and microstructure (SEM and XRD) of the obtained samples. Metakaolin (MK), is capable of accelerating either the dissolution or the condensation process (Essaidi et al., 2013), thereby increasing the chemical and mechanical performance of the hardened body. In this investigation, the amount of MK added to the unfired clay formulations was kept below 15 wt% to increase sustainability.

In order to rationalise the effect of the curing conditions (temperature and time) on the consolidation of the fresh pastes with untreated HC, a statistical approach was adopted. In particular, the results of ionic conductivity and density were studied using the statistical approach, ANOVA and Tukey–Kramer post hoc multiple comparisons tests (Oyar et al., 2018; Maaze and Shrivastava, 2023), in order to identify any significant correlation that could be used as indicators for a rapid scale-up of the consolidation process. Given the high rate of waste generation the in the mining and quarrying sector (Salemdeeb et al., 2016), the final objective of the research is to valorise two mining by-products from a circular economy perspective.

2. Materials and methods

2.1. Materials

The materials used as matrix for the formulations were:

a) Untreated halloysite (hereafter referred to as HC), a mining by-product obtained from industrial waste recovery processes for reuse as a secondary raw material. It is a by-product of the washing and filter-pressing process in the production of coarse to medium sized sands for the glass industry. It was sourced from the Province of Latina in Lazio, Italy, supplied by Sibelco Italia S.p.A., Maranello (MO), Italy. The batch of halloysite received was characterised in terms of the chemical and mineralogical components, with the grain size corresponding to that declared by the producer (Table 1). Chemical analysis by X-ray fluorescence gave the results shown in Table 1. The mineralogical composition analysis (mass %) performed on the sample reported the following values: 48 halloysite; 16 illite/smectite mixed layer; 13 plagioclase; 10 kaolinite; 9 quartz; 2 K-feldspar; 1 anatase; 1 goethite.
b) Fine sand (hereafter referred to as SA) is a by-product of the industrial production of quartz sand with a high silica content. The material is supplied by Sibelco Italia S.p.A., Maranello (MO), Italy, and processed at the Robilante plant, Robilante (CN), Italy. The specific chemical composition is also given in Table 1. The mineralogical composition (mass %) of the sample is: 67 of quartz, 27 of mica/illite, 6 of K-feldspar and minor amounts of iron oxides.
c) White metakaolin (hereafter referred to as MK), supplied by Backstain GmbH, Cologne, Germany, is a commercial high purity pozzolanic additive for OPC. It was amorphous except for traces of alpha-quartz. The specific chemical composition is also given in Table 1.

The range of variability reported in the product specification (technical data sheet) for the clay, sand and MK supplied are listed in Table 1. The variability in composition for each source mineral was due to its intrinsic natural variance. Table 1 also shows the particle size distribution with the values D50 (50% of the particles are smaller than the value indicated) and D90 (90% of the particles are smaller than the value indicated).

2.2. Sample preparation

The set of samples presented here was prepared with unfired halloysite in 50:50 ratio with sand and the addition of various percentages (0–15 mass%) of metakaolin. The alkali activator solution, NaOH 8 M, was added with a solid to liquid ratio of 100 to 150. The values of Si:Al molar ratio were in the range of 2.65–3.25, while Na:Al ratios were around 2.34–2.79. The latter values are consistent with the aim to create a highly alkaline environment capable of dissolving unfired clay. The amount of water was added after mixing the aluminosilicate powders and the alkaline solution to obtain a good viscosity of the fresh paste (for a solid/liquid ratio of about 1.5). Samples were cured at room temperature for 28 days. The same set of samples was tested under different temperature curing conditions, in a climatic chamber at 40, 60 and 70 °C and RH = 50% for 1, 3 and 7 days and then at room temperature for 28 days. Table 2 shows the formulations of the samples with and without MK, together with the oxide content and labelling system. It can be observed that the variation of the oxide content was minimal, so we can assume that the deviation in the geopolymerisation path was due to the different reactivity of the MK and halloysite powders.

2.3. Characterization methods

Mineralogical and chemical characterization of the batch of halloysite used specifically for this study was carried out using the Bruker S4

Table 1
Chemical composition (by XRF) and particle size of the three aluminosilicate powders used for the geopolymer pastes. The range of variation is taken from the technical data sheet (TDS).

Oxide (mass%)	Clay –HC TDS	Clay –HC XRF	Sand-SA TDS	Sand-SA XRF	Metakaolin-MK TDS	Metakaolin-MK XRF
SiO_2	52–55	53.3	83.5–86.5	85.1	50–55	53.3
Al_2O_3	23–30	27.4	7.5–10.5	8.7	43–47	40.5
Fe_2O_3	4–6.5	4.7	1–2	0.8	≤ 0.5	0.1
TiO_2	≤ 1	0.3	–	0.1	≤ 0.2	5.0
CaO	–	0.4	–	0.1	≤ 0.5	0.3
MgO	–	0.7	–	0.3	≤ 0.5	–
K_2O	–	1.8	2.8–4	3.7	≤ 0.5	0.6
Na_2O	–	1.4	–	–	≤ 0.5	–
LOI (%)	10	10.3	1.68	1.3	0.8	2.1
Sum		100.3		100.1		101.9
D50 (mm)	4.10 ± 0.1		8.29 ± 0.1		3.35 ± 0.1	
D90 (mm)	17.81 ± 0.1		23.26 ± 0.1		11.45 ± 0.1	

NaOH pellets (Sigma-Aldrich Corporation, Burlington, MA, USA, 98% purity) were dissolved in deionised water to prepare the 8 M sodium hydroxide solution.

Table 2
Formulations of the samples (S/L = solid to liquid weight ratio) and oxide content (mass %). $M_2O = K_2O + Na_2O$; MO=CaO + MgO, *Others* = all the other oxides from XRF data in Table 1.

Sample [a]	HC	SA	MK	S/L	SiO_2	Al_2O_3	M_2O	MO	Others	SUM
0MKX_Y	50	50	0	1.5	58	15	27	0.6	0.1	100.7
5MKX_Y	47.5	47.5	5	1.5	57	16	27	0.6	0.3	100.6
10MKX_Y	45	45	10	1.5	55	17	27	0.6	0.6	100.2
15MKX_Y	42.5	42.5	15	1.5	55	18	26	0.5	0.8	100.3

(a) Sample labelling: X = Temperature of curing (40 °C, 60 °C and 70 °C); Y = days of curing in temperature (1,3 and 7).

XRF spectrometer and the Bruker D8 Advance X-ray diffractometer, respectively.

As far as the geopolymer formulations are concerned, we first tested the samples with the integrity test, a preliminary qualitative test to assess the chemical/mechanical resistance of the material and its stability in an aqueous environment, just to verify that the geopolymerisation process had taken place. A piece of the sample was immersed in water with a solid/liquid ratio of 1:100, at room temperature (20 ± 5 °C), in static condition and for a duration of 24 h. After this time, the structural resistance and the integrity of the samples were evaluated, and the eluate was observed for colour and clarity.

Chemical stability in an aqueous environment was then determined by measuring the pH and ionic conductivity of the eluate solution. The pH and the ionic conductivity measurements were carried out by immersing a portion of the sample in deionised water with a solid/liquid ratio of 1/10 for 24 h under stirring conditions at 20 ± 2 °C. The ionic conductivity and pH of the eluate solutions were determined at different times (0, 5, 15, 30, 60, 120, 240, 360, 1440 min) in order to obtain a trend of the change in value during the 24 h and to have information on the amount of dissolved solids. The pH was determined with a Hamilton type Liq-glass SL Laboratory pH sensor (Hamilton A.G., Bonaduz, Switzerland) and the ionic conductivity of the solution was measured with a calibrated cell, both connected to the pH 5/6 and Ion 6 digital display of Oakton Instruments, Vernon Hills, IL, USA.

Measurements of skeletal density by helium pycnometry were performed on solid samples using Micromeritics Accupyc II 1340. The tests were repeated in triplicate and averages are given below (Fig. 3).

X-ray diffraction patterns of the produced geopolymers were recorded using a PW3710 diffractometer (Philips, Almelo, The Netherlands) operated at room temperature. The samples were scanned in the 2Θ range of 5–70° on powdered samples (grain diameter <20 μm) using Cu-Kα 1.5406 Å radiation from a conventional X-ray source operated at 35 kV, 35 mA, a scan step of 0.02°. The patterns were analysed using the High Score Plus (PANAlytical) software. The XRD patterns of the starting aluminosilicate powders are given for comparison (Fig. 6).

Morphological observations were made on fresh fractured samples by environmental scanning electron microscopy (ESEM) using a QUANTA 200 microscope equipped with EDS (FEI, Hillsboro, OR, USA). The planar surface of the sample was placed on an Al specimen holder with the silver glue and, after drying, the surface was gold coated prior to analysis.

2.4. Statistical analysis

To test whether the parameters of the curing process as well as the MK content had an influence on the ionic conductivity and/or density values, firstly a 3-way ANOVA (factor1: MK content; factor2: curing temperature; factor3: curing time; $p < 0.05$) was performed, followed by Tukey-Kramer post hoc test ($p < 0.05$).

Then, to investigate the type of relationship (in terms of linearity or non-linearity) between each of these factors and each of the properties of interest, the value of R^2 obtained from a simple linear regression was compared with that obtained from a quadratic regression.

Finally, to build a unique statistical model that could predict the properties of the resulting compound, considering the three parameters of the curing process (and possibly their interactions), we fitted a Generalized Linear Model (GLM) with a stepwise selection of the features. This procedure allowed an automated selection of the features to be included in the model: each parameter was added to the model if it significantly improved the goodness of fit (in terms of deviance) and it was removed if it did not. For the present work, the initial model included a constant term (intercept), a linear term for each parameter of the curing process and all products of pairs of distinct factors (i.e., interactions between 2 factors in the form factor1*factor2). The upper bound was a model that also included the quadratic term for each factor, since quadratic regression outperformed the linear regression. Note that we did not set a lower bound for the model, so the algorithm could arbitrarily remove terms from the initial model until it was left with only one constant term. Conversely, the resulting model (automatically fitted) could not be more complex than the one we set as the upper bound. All analyses were performed with custom MATLAB scripts (Mathworks Inc.; *polyfit* function was used to perform the regressions; *stepwiseglm* function with default parameters was used to build the GLMs).

3. Results and discussion

3.1. Chemical stability and density of the hardened geopolymers

In preliminary experiments, it was found that curing at temperatures slightly above room temperature, between 40 and 80 °C, favoured the onset of the alkali activation process and apparently conferred better structural strength, but in this case it was not sufficient to achieve a good stability, especially in water. In fact, when the samples were immersed in water (solid:liquid ratio 1:10), they began to lose mass and showed low stability (Sgarlata, 2022).

A significant improvement in terms of chemical stability was observed when a quantity of MK was added to the untreated clay. Positive results were only obtained when the samples were cured for at least 7 days at a temperature of 40–60 °C and a relative humidity of around 50%, similar to previous studies (Khaled et al., 2023). Regarding the integrity test, almost all the samples resisted in water, especially the samples with thermal curing longer than 3 days.

In order to assess the chemical stability in the aqueous environment of the material and to evaluate the effectiveness of the consolidation process on the samples that passed the integrity test, the pH and ionic conductivity tests were carried out. The ionic conductivity and pH of the eluate solutions were determined at different times (0, 5, 15, 30, 60, 120, 240, 360, 1440 min) in order to obtain a trend of the change in value during the 24 h and to have information on the amount of dissolved solids. The results showed that the pH values remained fairly constant between 10.2 and 11 for the duration of the test confirming an alkaline chemical stability of the material (Aly et al., 2008; Luna Galiano et al., 2011; Lancellotti et al., 2013), as shown in Fig. 1 for 0MK_60_3 and 15MK_60_3, as examples to show the trend of the measurements during of the first 24 h of the test.

Fig. 1b shows the ionic conductivity of two samples, as representative of all the groups (see details in Fig. 2). The ionic conductivity of the eluates provides additional information, with respect to pH, on the ionic species leached out from the geopolymer matrix. The Na^+ ions of the unreacted alkaline activator solution are included in the ionic conductivity measurements but not in the pH values, as the pH is sensitive to the leaching of unreacted OH- groups and the ionic exchange of H+ from the

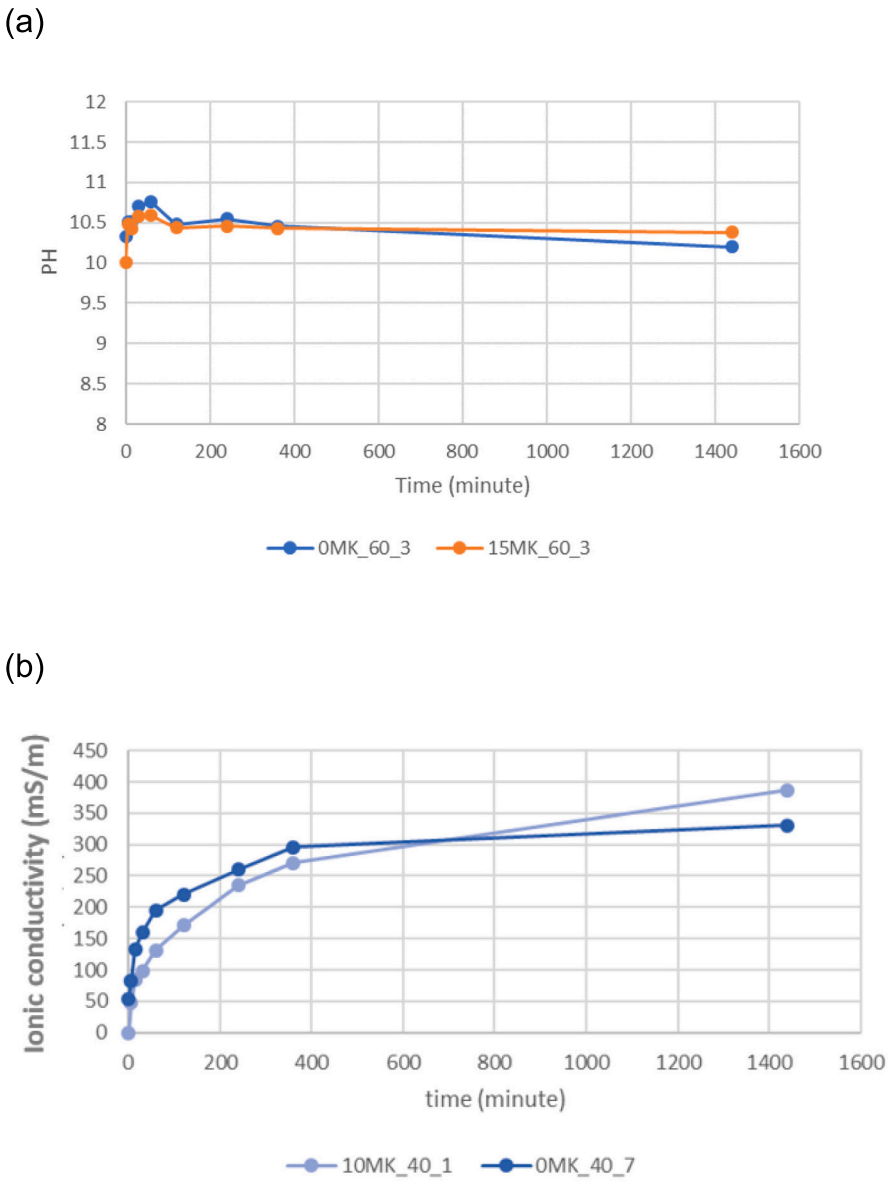

Fig. 1. Example of pH measurements for 0MK_60_3 and 15MK_60_3 (a) and trend curve of ionic conductivity of 10MK-40-1 and 0MK-40-7 (b). The confidence interval is about 1% for pH and 2% for ionic conductivity.

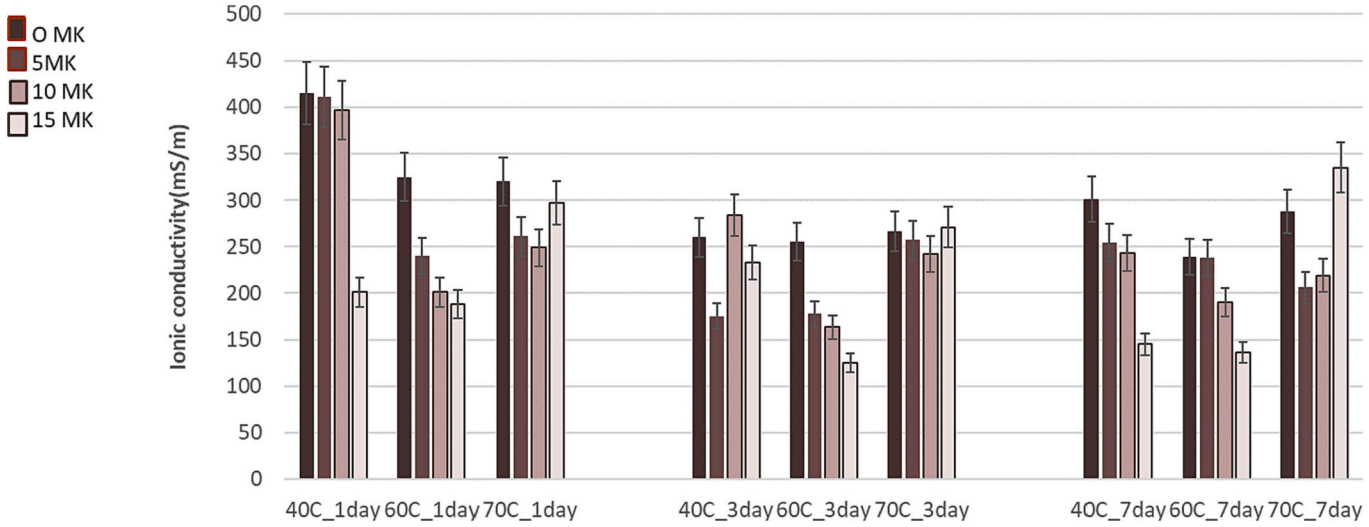

Fig. 2. Histogram of ionic conductivity of all samples compared.

deionised water for Na + in the geopolymer gel (Sgarlata, 2022).

Fig. 2 shows the ionic conductivity for all samples, grouped by curing time and temperature. The colours indicate the MK content. The maximum values do not exceed 400 mS/m, a figure that indicates a good degree of reticulation for clayey powders (Sgarlata et al., 2021). It was evident that complex interactions between these three parameters influenced the final conductivity of the samples. It appears that the conductivity decreases with increasing curing time, with better results (i.e. lower values) for thermal curing longer than 1 day. The temperature of the climate chamber also seems to influence the consolidation of the samples, with curing at 60 °C giving the best samples. Higher conductivity values, indicating poorer consolidation, were obtained at the lowest temperature (40 °C) and shorter times (1 day). The values at 40 °C for 1 day were 415 mS/m for 0MK_40_1, 411 mS/m for 5MK_40_1, 397 mS/m for 10MK_40_1 and 201 mS/m for 15MK_40_1 compared to 301 mS/m for 0MK_40_7, 254 mS/m for 5MK_40_7, 243 mS/m for 10MK_40_7, and 145 mS/m for 15MK_40_7. There is a visible decrease in the values as curing time increases. No evident differences were found between samples cured at 60 and 70 °C, but the best results were obtained at a temperature of 60 °C and a curing time of 3 days, with 255 mS/m for 0MK_60_3, 177 mS/m for 5MK_60_3, 163 mS/m for 10MK_60_3, and 125 mS/m for 15MK_60_3. Fig. 2 shows all the samples signed in different colours according to the % of metakaolin, and it is clearly visible this reduction in value with the increase in %MK, especially at 40 °C and 60 °C. These results are comparable to those obtained for samples containing calcined clay (Sgarlata et al., 2021), demonstrating that a small amount of highly reactive aluminosilicate, such as metakaolin, avoids the need for thermal treatment of the main clay component. These aspects will be further examined in the following paragraphs.

Skeletal density is shown in the histogram in Fig. 3. The effect of the curing temperature on the density values is quite remarkable, with a positive correlation and independent of the curing time. In addition, the density tends to decrease with the increase of %MK. The samples with lower densities are those with 15% MK at 60 and 40 °C, probably due to the higher presence of porosity compared to the other samples (with higher density probably due to the presence of undissolved phases).

3.2. *Influence of different variables on ionic conductivity*

We wanted to test the statistical significance of the effects already observed in the histograms (Figs. 2 and 3). The variance analysis by ANOVA was adopted as already reported in the literature to correlate compositional features with material performance (Oyar et al., 2018.; Maaze and Shrivastava, 2023).

Firstly, it was investigated whether the MK content and the

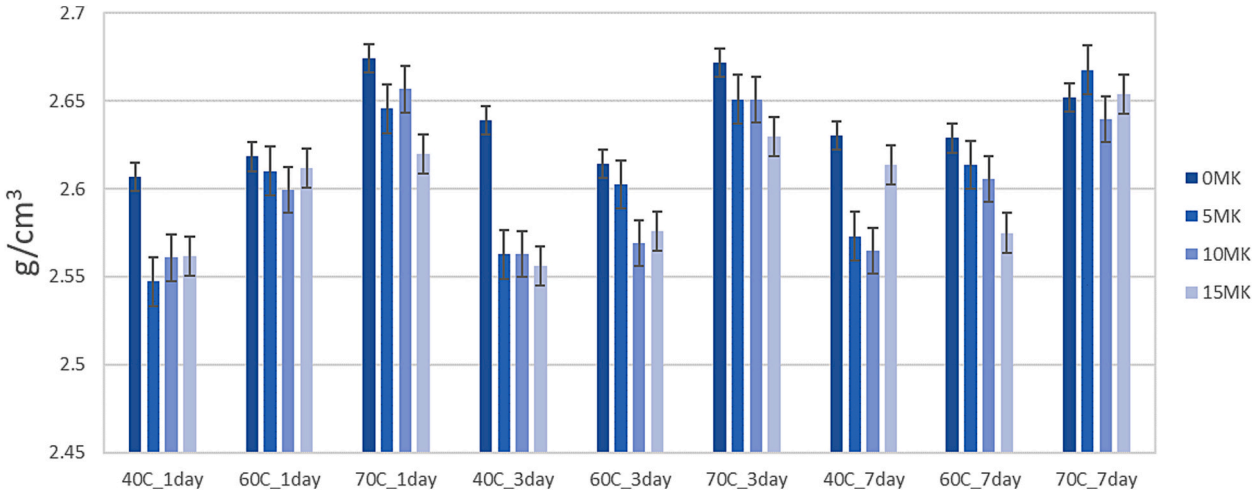

Fig. 3. Histogram of skeletal density of all samples compared.

parameters of the curing process (namely the temperature and the duration) had an influence on the final ionic conductivity of the eluate. The 3-way ANOVA showed that all three factors significantly influenced the ionic conductivity ($p < 0.05$). In addition, the interaction between MK content and curing temperature was also significant ($p < 0.05$, see Table 3 and Fig. 4a). In particular, statistically significant differences for the conductivity were found between the group with 0% MK with the higher values, and the group with 15% MK with lower values (Tukey-Kramer post hoc test, $p < 0.05$), as shown in Table 3.

In term of temperature, statistically significant differences were found between the group cured at 60 °C and the other two groups cured at 40 and 70 °C (Tukey-Kramer post hoc test, $p < 0.05$), as reported in Table 3.

Statistically significant differences were found between the group with curing time of 1 day and the other two groups with curing time of 3 and 7 days (Tukey-Kramer post hoc test, $p < 0.05$; Table 3).

Finally, statistically important differences were found for the interaction between %MK and curing temperature. As shown in Fig. 4a, the formulation with 15% of MK cured at 60 °C (15MK_60_X) has the lowest conductivity.

The relationships between each curing parameter and the final conductivity were non-linear. In fact, the quadratic regression tended to outperform the linear regression in terms of R^2 values (quadratic R^2: 0.16 for %MK; 0.20 for curing temperature (curing temp); 0.18 for curing time vs. linear R^2: 0.16 for %MK; 0.02 for curing temp; 0.09 for curing time). We decided to exploit the automatic selection of variables allowed by the stepwise procedure to create a single model that could explain conductivity better than the single models fitted on the individual parameters.

Considering that all three parameters (MK%, curing temperature, curing time) had an influence on conductivity (see ANOVA results) and that the quadratic fitting appeared more appropriate than the linear one, we built a stepwise GLM that could include a constant term, the three parameters (MK%, temperature, time), their (multiplicative) interactions, and the three parameters squared.

After the fitting phase, the resulting GLM followed the equation:

$$\begin{aligned}\text{Conductivity}(\text{mS/m}) = {} & +\mathbf{1519}\text{–}\mathbf{17.5}^{*}\,\text{MK}(\%) - \mathbf{39.3}^{*}\,\text{temp}(^{\circ}\text{C}) \\ & - \mathbf{84.2}^{*}\text{time}(\text{days}) + \mathbf{0.22}^{*}\,\text{MK}^{*}\text{temp} \\ & + \mathbf{0.5}^{*}\,\text{temp}^{*}\text{time} + \mathbf{0.32}^{*}\,\text{temp}^{2} + \mathbf{5.7}^{*}\,\text{time}^{2}\end{aligned}$$

With these estimates, the model scored an R^2 equal to 0.64, well predicting the final conductivity of the compound. In Fig. 5a, the conductivity values predicted by the model based on the preparation process parameters are plotted against the actual final values (points laying on the diagonal indicate perfect predictions). In the model, the coefficients of the interactions (MK * temp and temp * time) were not significant in a 'strict' sense ($p = 0.061$ and $p = 0.058$, respectively), but they greatly improved the fit of the model ($R^2 = 0.54$ for the model fitted without the interaction terms), so we allowed them to be included in the model.

Table 3
Ionic conductivity and density values are grouped according to the MK content, curing temperature and curing time. Group mean values and confidence intervals from the ANOVA are reported.

		Ionic conductivity (mS/m)	Density (g/cm^3)
MK content (wt%)	0	296.7 (± 29.2)	2.637 (± 0.0091)
	5	246.6 (± 29.2)	2.608 (± 0.0091)
	10	244.1 (± 29.2)	2.601 (± 0.0091)
	15	214.6 (± 29.2)	2.595 (± 0.0091)
Curing temp (°C)	40	276.6 (± 22.7)	2.58 (± 0.0071)
	60	206.5 (± 22.7)	2.60 (± 0.0071)
	70	268.4 (± 22.7)	2.65 (± 0.0071)
Curing time (days)	1	292.1 (± 22.7)	2.61 (± 0.0071)
	3	226.5 (± 22.7)	2.61 (± 0.0071)
	7	232.9 (± 22.7)	2.61 (± 0.0071)

3.3. Influence of different variables on density

It was investigated whether the MK content and the parameters of the curing process (namely the temperature and time) also had an influence on the final density of the compound. The 3-way ANOVA showed that the MK content and curing temperature had a significant effect on density ($p < 0.05$). In addition, the interaction between MK content and temperature was also marginally significant ($p < 0.05$; Fig. 4c and Table 3). In particular, statistically significant differences in the density were found between the 0% MK group and the other groups (5% MK, 10% MK and 15% MK) (Tukey-Kramer post hoc test, $p < 0.05$), as shown in Table 3. The density values decrease with the MK content.

A gradual, significant increase in density values was observed with increasing curing temperature (Table 3; Tukey-Kramer post hoc test, $p < 0.05$), whereas curing time had no effect on the density. Accordingly, the ranges of density values in Table 3 for the different time groups are highly overlapping.

Finally, statistically significant differences were found from the % MK*curing temperature interaction (Fig. 4b). For example, the 5MkTemp60 group density differed from 5MkTemp40, 10MkTemp40, 15MkTemp40 (with a lower density), but also from 0MkTemp70 and 5MkTemp70 (with a higher density, Tukey-Kramer post hoc test, $p < 0.05$).

The relationships between MK/curing temperature and final density were non-linear, with a quadratic regression outperforming the linear regression in terms of R^2 values (quadratic R^2: 0.19 for %MK; 0.66 for curing temp vs. linear R^2: 0.16 for %MK; 0.60 for curing temp). The R^2 values for the regression between curing time and final density were extremely low according to ANOVA results (quadratic R^2: 0.007; linear R^2: 0.004), because varying the curing time had no effect on the density of the compound.

Considering these results, the quadratic fitting appears more appropriate than the linear fit for the GLM statistical elaboration.

To obtain a unique model that could predict the density of the final compound, we again fitted a GLM using the stepwise procedure. As already done for the conductivity, we included in the model a constant term, the 3 parameters (MK%, temperature, time), their (multiplicative) interactions and the 3 parameters squared. Note that, as a double check, we allowed the model to include the time parameter, even though the results presented so far indicated that it was significant in determining the final density of the material. After the fitting phase and the automatic selection of the relevant features, we obtained the following equation:

$$\begin{aligned}\text{Density}\left(\text{g/cm}^3\right) = {} & +\mathbf{2.852}\text{–}\mathbf{6.1}^{*}\mathbf{10}^{-3^{*}}\,\text{MK}(\%) - \mathbf{1.1}^{*}\mathbf{10}^{-2^{*}}\,\text{temp}(^{\circ}\text{C}) \\ & + \mathbf{2.3}^{*}\mathbf{10}^{-4^{*}}\,\text{MK}^{2} + \mathbf{1.2}^{*}\mathbf{10}^{-4^{*}}\,\text{temp}^{2}\end{aligned}$$

With these estimates, the model achieved an R^2 equal to 0.85 and predicted the final density of the compound well, as shown in Fig. 5b.

Furthermore, in accordance with the ANOVA and the regression results, the curing time terms were removed from the final model as they did not significantly affect the density. The non-linear relationships were confirmed by the presence of the quadratic terms (MK^2 and $temp^2$), while the MK*temp interaction, which was marginally significant in the ANOVA, was here removed.

3.4. XRD and SEM characterization of hardened geopolymers

In order to observe possible mineralogical variations with the curing temperature of the MK addition, all samples were analysed by X-ray diffraction. Fig. 6 shows the comparison of the spectra of the samples

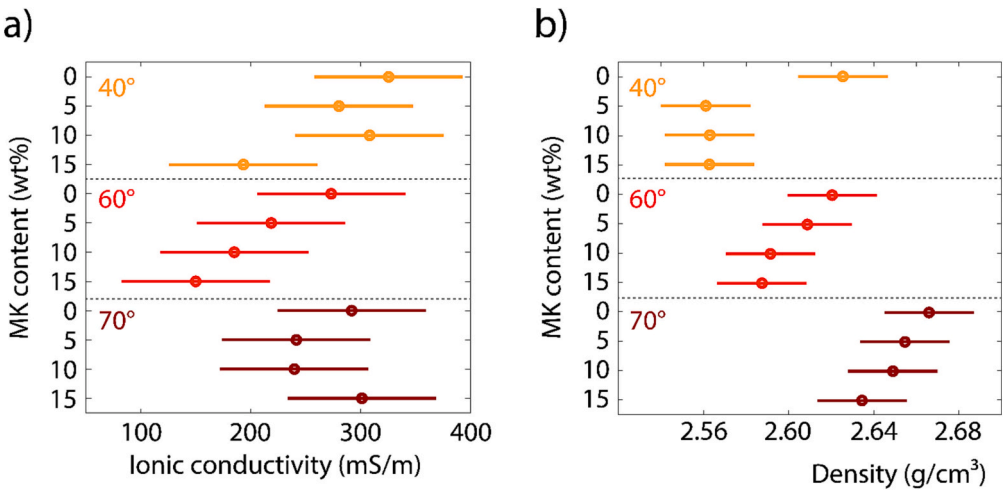

Fig. 4. Multiple comparison of sample marginal means to assess the effect of curing parameters on: (a) ionic conductivity and (b) density. Values are grouped according to the interaction between MK content and temperature. The circles represent the mean values and the bars the confidence intervals of each group.

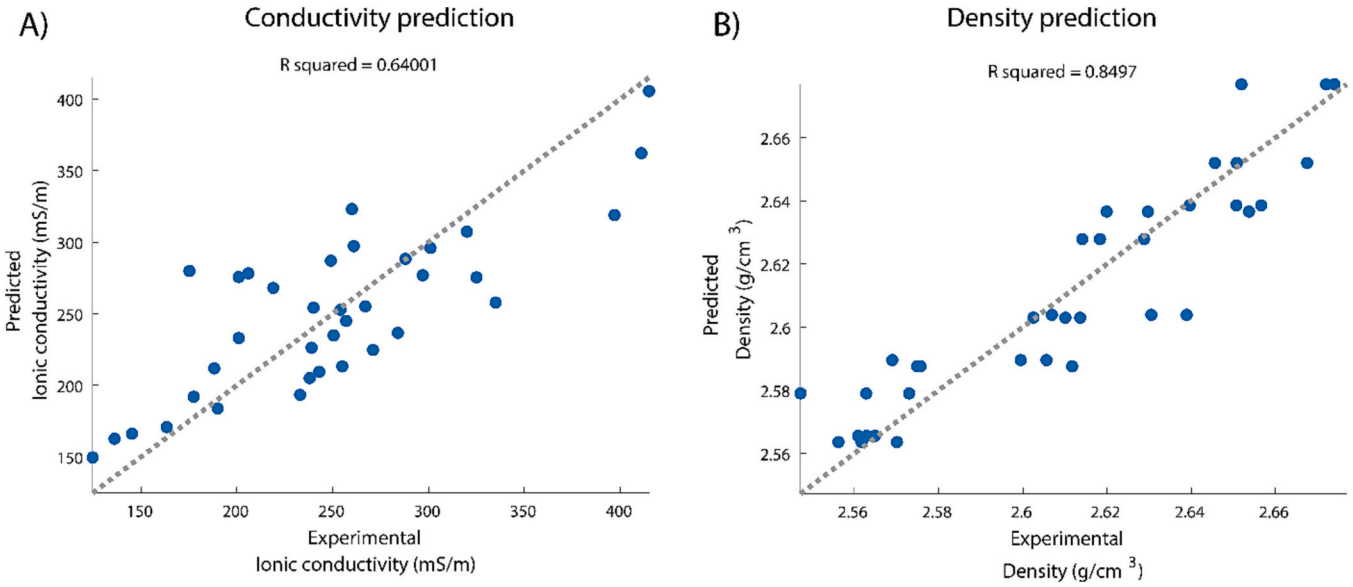

Fig. 5. Predicted vs real conductivity values (a) and real density values (b). Blue dots represent conductivity values predicted by the fitted GLM vs their experimentally measured counterparts. The dotted line is the diagonal representing perfect predictions. (For interpretation of the references to colour in this figure legend, the reader is referred to the web version of this article.)

with the different percentages of MK added, cured for 3 days at 40 °C (a), 60 °C (b) and 70 °C (c). The XRD patterns of the starting powders (HC, SA and MK) have also been added for comparison.

The main peaks indicate the presence of quartz (ICSD 01–085-0796), illite (ICSD 00–002-0050), halloysite (ICSD 00-29-1487) and kaolinite (ICSD 00–001-0527) as the main minerals present in the clay (HC) and in the sand (SA). It is difficult to discern significant changes in the mineralogy of the samples when comparing the patterns of the source materials with those of the geopolymers. As a general trend, it can be affirmed that the alkali activation process decreased the crystallinity of the illite and kaolinite phases with the disappearance of the peaks (below 20° in 2Θ). On the contrary, the peaks of the feldspars became more visible in the 2Θrange 20–32°. The same observation applies for the smectite-type T-O-T phyllosilicate which became more prominent. The absence of a peak below 20° in 2Q makes their identification impossible.

In the range between 15° and 35° 2θ there is a slight increase in the amplitude of the spectral band, probably due to the increase in the amorphous geopolymer phase with the addition of MK, which is more visible in samples cured at 70 °C (Melele et al., 2018; Douiri et al., 2017; Fernández-Jiménez et al., 2008).

It is difficult to detect significant differences in the spectra of samples with different MK percentages or different curing temperatures, they are very similar. No new crystalline phases, such as zeolites (Juengsuwattananon and Pimraksa, 2017), were found in the samples.

The SEM analysis was carried out on specimens that gave the best and worst results in previous tests to show how the texture of the densified materials changed.

The SEM micrographs shown in Fig. 7 belong to 0MK40_3 (a) and 15MK40_3 (b). The argillaceous platelets visible in the micrograph 7*a* showed a loose matrix, not reticulated, indicating that the curing condition was not sufficient to produce reticulation or densification. This very loose aspect of the aluminosilicate powder was predictive of its high and efficient dispersion in the alkali activated paste and good workability. In the micrograph 7*b* of samples with 15% MK cured at 40 °C the morphology of the matrix seems to have changed only,

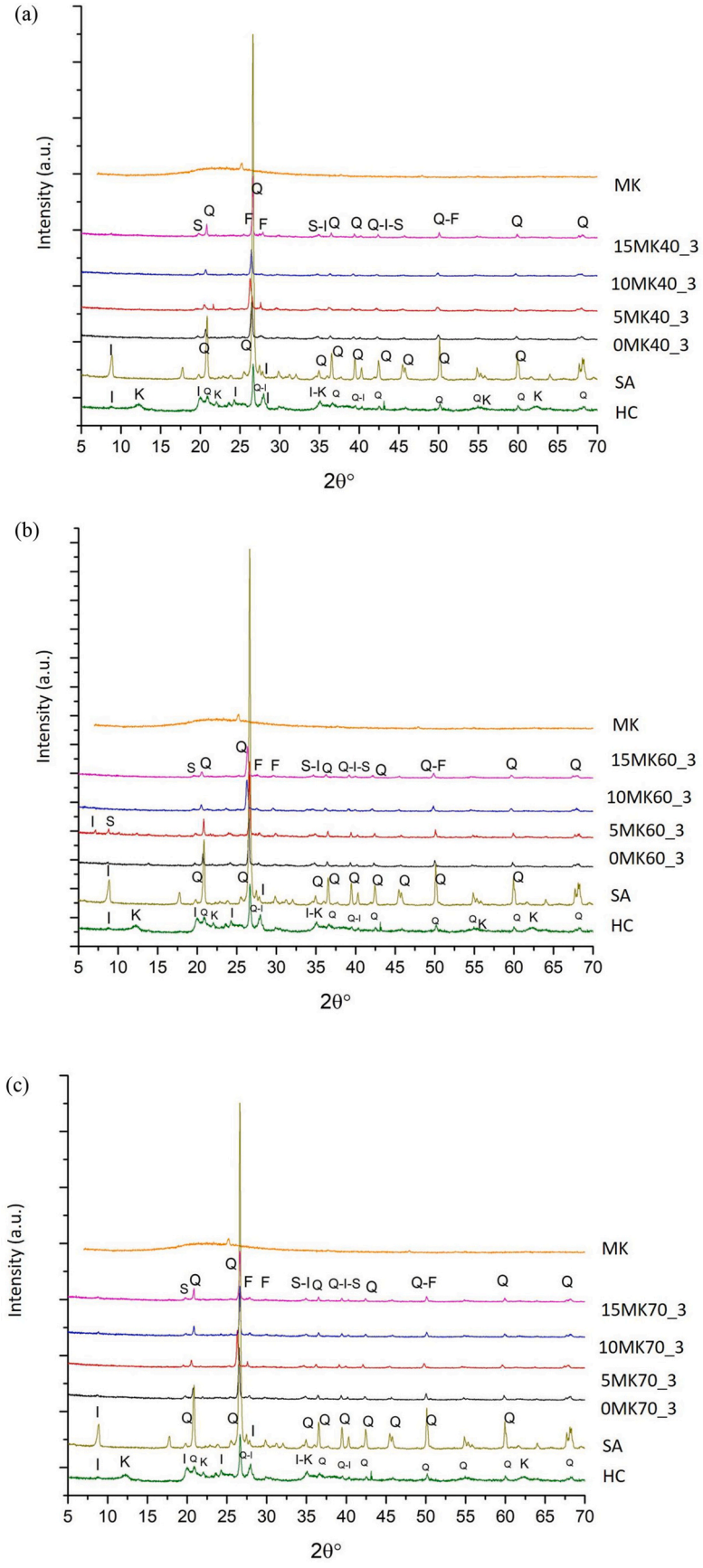

Fig. 6. XRD of samples cured for 3 days at 40 °C (a), 60 °C (b) and 70 °C (c). (K: Kaolinite/Halloysite (7 Å); I: Illite; Q: Quartz; S: Smectite; F: Feldspars).

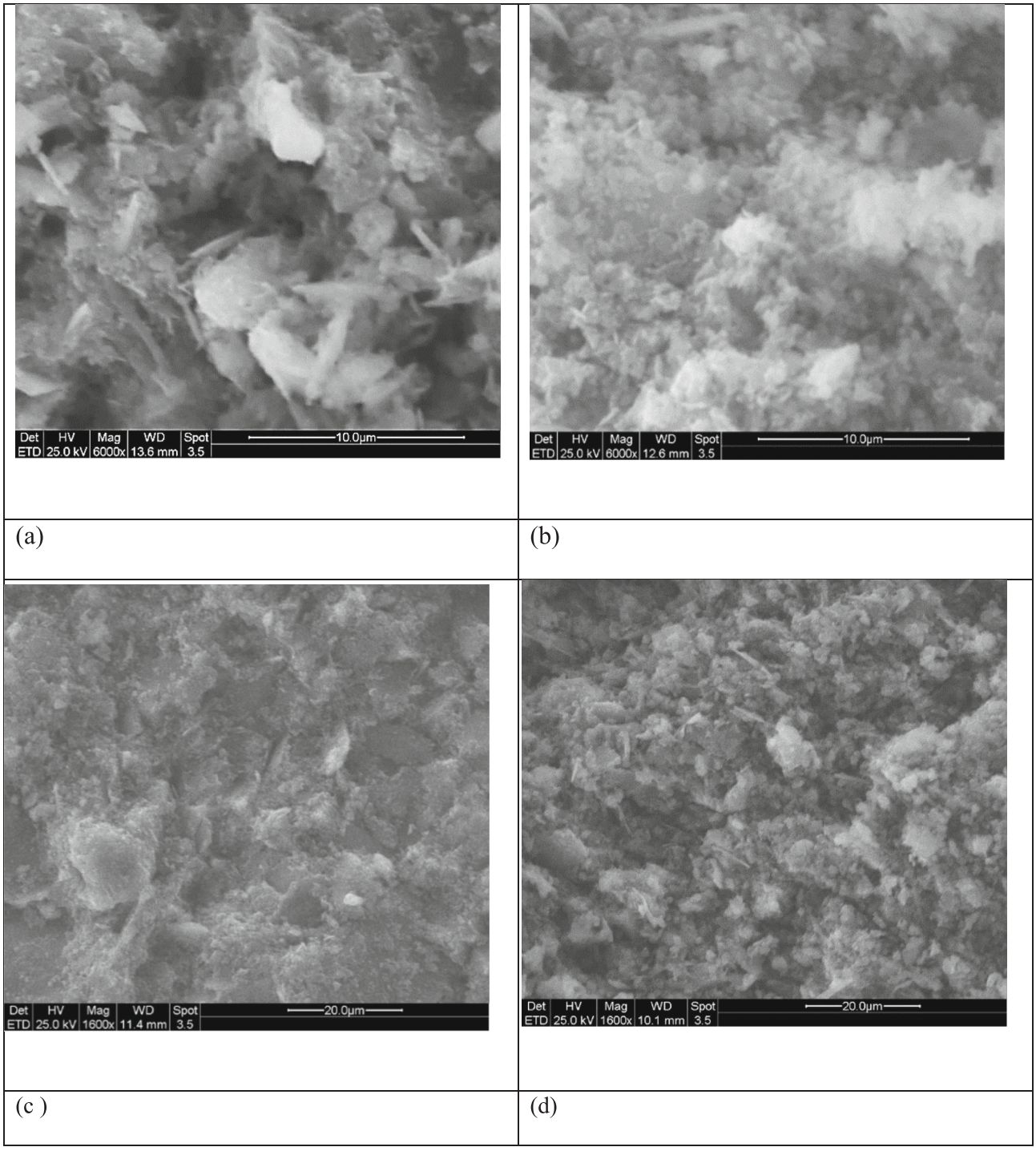

Fig. 7. SEM images of 0MK40_3 (a) and 15MK-40_3 (b), 0MK60_3 (c) and 15MK60_3 (d).

appearing more compact than 0MK40_3.

Fig. 7*c* and *d* are show the SEM micrographs of 0 and 15% MK samples cured at 60 °C for 3 days. The morphology of the matrix with 0% MK appears denser and more compact compared to the matrix of 0MK40_3, suggesting the improvement obtained by increasing the curing temperature at 60 °C.

4. Conclusion

The reuse of mineral wastes and by-products was investigated to produce more sustainable binders by alkali activation at room temperature or at 40 and 60 °C to maintain a high level of sustainability. Attention was focused on the influence of the temperature on the geopolymerisation process, as well as the effects on the microstructure of the samples obtained with untreated clay. In particular, the best results were obtained with the combination of halloysite by-product (HC) and silica sand by-product (SA), also optimised with the addition of a small percentage of metakaolin (MK). The curing temperature of this mix, which has been shown to give good reticulation, is above 25 °C, i.e. between 40 and 60 °C, and it is influenced by the curing time. Better results were obtained with a curing time of >3 days in a climatic chamber with controlled temperature and relative humidity. The

increase of MK in the clay mixtures favours the reticulation process. The latter results were confirmed by the statistical approach used. The use of simple NaOH as an activator solution, without sodium silicate, could be an advantage in terms of further sustainability of these materials.

In conclusion, it has been statistically demonstrated how the addition of fillers, an easily controllable industrial step, can maximise the performance of the consolidated material, rather than controlling the curing time and temperature conditions. In addition, the use of a test as simple as measuring the ionic conductivity of the water eluate to separate good formulations from unstable ones based on a minimum conductivity value appears to be a sensitive measurement in the case of alkali activated materials.

CRediT authorship contribution statement

Caterina Sgarlata: Data curation, Investigation. **Francesco Edoardo Vaccari:** Formal analysis, Software, Visualization, Writing – review & editing. **Alessandra Formia:** Methodology, Supervision. **Francesco Ferrari:** Funding acquisition, Supervision. **Cristina Leonelli:** Conceptualization, Supervision, Writing – review & editing.

Declaration of competing interest

The authors declare that they have no known competing financial interests or personal relationships that could have appeared to influence the work reported in this paper.

Data availability

Data will be made available on request.

References

Almas, K., Rao, B.D.V.C.M., Yadav, M.J., Giri, P.S.N.R., 2021. Performance studies on limestone calcined clay based concrete. IOP Conf. Ser.: Mater. Sci. Eng. 1091, 012076.

Aly, Z., Vance, E.R., Perera, D.S., Hanna, J.V., Griffith, C.S., Davis, J., Durce, D., 2008. Aqueous leachability of metakaolin-based geopolymers with molar ratios of Si/Al = 1.5–4. J. Nucl. Mater. 378, 172–179.

Blouch, N., Rashid, K., Zafar, I., Ltifi, M., Ju, M., 2023. Prioritization of low-grade kaolinite and mixed clays for performance evaluation of Limestone Calcined Clay Cement (LC3): Multi-criteria assessment. Appl. Clay Sci. 243, 107080.

Douiri, H., Louati, S., Baklouti, S., Arous, M., Fakhfakh, Z., 2017. Structural and dielectric comparative studies of geopolymers prepared with metakaolin and Tunisian natural clay. Appl. Clay Sci. 139, 40–44.

Duxson, P., Provis, J.L., Lukey, G.C., Mallicoat, S.W., Kriven, W.M., van Deventer, J.S.J., 2005. Understanding the relationship between geopolymer composition, microstructure and mechanical properties. Colloids Surf. A: Physicochem. Eng. Aspects 269, 47–58.

Esaifan, M., Rahier, H., Barhoum, A., Khoury, H., Hourani, M., Wastiels, J., 2015. Development of inorganic polymer by alkali-activation of untreated kaolinitic clay: reaction stoichiometry, strength and dimensional stability. Constr. Build. Matls. 91, 251–259.

Essaidi, N., Samet, B., Baklouti, S., Rossignol, S., 2013. Effect of calcination temperature of Tunisian clays on the properties of geopolymers. Ceramics-Silikáty 57 (3), 251–257.

Fernandez, R., Martirena, F., Scrivener, K.L., 2011. The origin of the pozzolanic activity of calcined clay minerals: a comparison between kaolinite, illite and montmorillonite. Cem. Concr. Res. 41, 113–122.

Fernández-Jiménez, A., Monzó, M., Vicent, M., Barba, A., Palomo, A., 2008. Alkaline activation of metakaolin–fly ash mixtures: obtain of zeoceramics and zeocements. Microporous Mesoporous Matls 108, 41–49.

Juengsuwattananon, K., Pimraksa, K., 2017. Variable factors controlling amorphous-zeolite phase transformation in metakaolin based geopolymer. Acta Metall. Slovaca 23, 378–386.

Khaled, Z., Mohsen, A., Soltan, A.-M., Kohail, M., 2023. Optimization of kaolin into Metakaolin: Calcination Conditions, mix design and curing temperature to develop alkali activated binder. Ain Shams Eng. J. 14, 102142.

Kóth, J., Sinkó, K., 2023. Geopolymer Composites—in Environmentally Friendly Aspects. Gels 9, 196.

Lancellotti, I., Ponzoni, C., Barbieri, L., Leonelli, C., 2013. Alkali activation processes for incinerator residues management. Waste Manag. 33, 1740–1749.

Lothenbach, B., Scrivener, K., Hooton, R.D., 2011. Supplementary cementitious materials. Cem. Concr. Res. 41, 1244–1256.

Luna Galiano, Y., Fernández Pereira, C., Vale, J., 2011. Stabilization/Solidification of a municipal solid waste incineration residue using fly ash-based geopolymers. J. Hazard. Mater. 185, 373–381.

Maaze, M.R., Shrivastava, S., 2023. Design optimization of a recycled concrete waste-based brick through alkali activation using Box- Behnken design methodology. J. Build. Eng. 75, 106863.

Melele, S.J.K., Tchakouté, H.K., Banenzoué, C., Kamseu, E., Rüscher, C.H., Andreola, F., Leonelli, C., 2018. Investigation of the relationship between the condensed structure and the chemically bonded water content in the poly(sialate-siloxo) network. Appl. Clay Sci. 156, 77–86.

Oyar, P., Asghari Sana, F., Durkan, R., 2018. Comparison of mechanical properties of heat-polymerized acrylic resin with silver nanoparticles added at different concentrations and sizes. J. Appl. Polym. Sci. 135 (6), 45807.

Salemdeeb, R., Al-Tabbaa, A., Reynolds, C., 2016. The UK waste input–output table: linking waste generation to the UK economy. Waste Manag. Res. 34, 1089–1094.

Scrivener, K., Martirena, F., Bishnoi, S., Maity, S., 2018. Calcined clay limestone cements (LC3). Cem. Concr. Res. 114, 49–56.

Sgarlata, C., 2022. Study of Sustainable Geopolymer Formulations. Ph.D. Thesis in Industrial Engineering,. University of Modena and Reggio Emilia, Modena, Italy (in English).

Sgarlata, C., Formia, A., Ferrari, F., Leonelli, C., 2021. Effect of the introduction of reactive fillers and metakaolin in waste clay-based materials for geopolymerization processes. Molecules 26, 1325.

Sgarlata, C., Formia, A., Siligardi, C., Ferrari, F., Leonelli, C., 2022. Mine clay washing residues as a source for alkali-activated binders. Materials 15, 83.

Slaty, F., Khoury, H., Wastiels, J., Rahier, H., 2013. Characterization of alkali activated kaolinitic clay. Appl. Clay Sci. 75–76, 120–125.

Tchakoute Kouamo, H., Mbey, J.A., Elimbi, A., Kenne Diffo, B.B., Njopwouo, D., 2013. Synthesis of volcanic ash-based geopolymer mortars by fusion method: effects of adding metakaolin to fused volcanic ash. Ceram. Int. 39, 1613–1621.

Wan, Q., Rao, F., Song, S., García, R.E., Estrella, R.M., Patiño, C.L., Zhang, Y., 2017. Geopolymerization reaction, microstructure and simulation of metakaolin-based geopolymers at extended Si/Al ratios. Cem. Concr. Compos. 79, 45–52.

Yousef, R.I., El-Eswed, B., Alshaaer, M., Khalili, F., Rahier, H., 2012. Degree of reactivity of two kaolinitic minerals in alkali solution using zeolitic tuff or silica sand filler. Ceram. Int. 38, 5061–5067.

Zhang, Z., Provis, J.L., Wang, H., Bullen, F., Reid, A., 2013. Quantitative kinetic and structural analysis of geopolymers. Part 2. Thermodynamics of sodium silicate activation of metakaolin. Thermochim. Acta 565, 163–171.

Žibret, L., Wisniewski, W., Horvat, B., Božič, M., Gregorc, B., Ducman, V., 2023. Clay rich river sediments calcined into precursors for alkali activated materials. Appl. Clay Sci. 234, 106848.